Supporting Information

Synergistic vacancy defect and bandgap engineering in Ag/S co-doped Bi_2O_3-based sulfur oxide catalyst for efficient hydrogen evolution

Zhengjie Su[1], Xinru Wu[1], Dong-Hau Kuo[2,*], Baoqian Yang[1], Binghong Wu[1], Longyan Chen[1], Pengkun Zhang[1], Jinguo Lin[1,*], Xiaoyun Chen[1,*], Dongfang Lu[1,*]

[1] College of Materials Engineering, Fujian Agriculture and Forestry University, Fuzhou 350002, China

[2] Department of Materials Science and Engineering & Graduate Institute of Energy and Sustainability Technology, National Taiwan University of Science and Technology, Taipei 10607, Taiwan

*Corresponding author

E-mail address: dhkuo@mail.ntust.edu.tw (D. H. Kuo)

E-mail address: fjldf@126.com (D. Lu)

E-mail address: fjlinjg@126.com (J. Lin)

E-mail address: fjchenxy@126.com (X. Chen)

Experimental Section

1. Apparent quantum efficiency computation

According to the literature reports [1-3] for measuring the apparent quantum efficiency (AQE). The experiment was measured under the photocatalytic reaction conditions of monochromatic light of 420 nm (λ), average radiation intensity (I) of 2.87 mW/cm^{-2}, and irradiation area (A) of 40.12 cm^2. The total H_2 evolution with 50 mg of Ag/S-Bi_2O_3 catalyst was 378.6 μmol, which can be used to determine the reacted photons (N_{reac}). The number of photons (N_{in}) illuminated to the reactor is computed according to the following equations:

$$N_{in} = \frac{E \times \lambda}{h \times \mathrm{c}} = \frac{A \times I \times t \times \lambda}{h \times c} = \frac{40.12 \times 2.87 \times 10^{-3} \times 3600 \times 6 \times 420 \times 10^{-9}}{6.626 \times 10^{-34} \times 3 \times 10^{8}} = 5.255 \times 10^{21}$$

$$\mathrm{AQE} = \frac{N_{reac}}{N_{in}} \times 100\% = \frac{2 \times 6.02 \times 10^{23} \times 378.6 \times 10^{-6}}{5.255 \times 10^{21}} \times 100\ \% = 8.67\ \%$$

Additional figures and tables

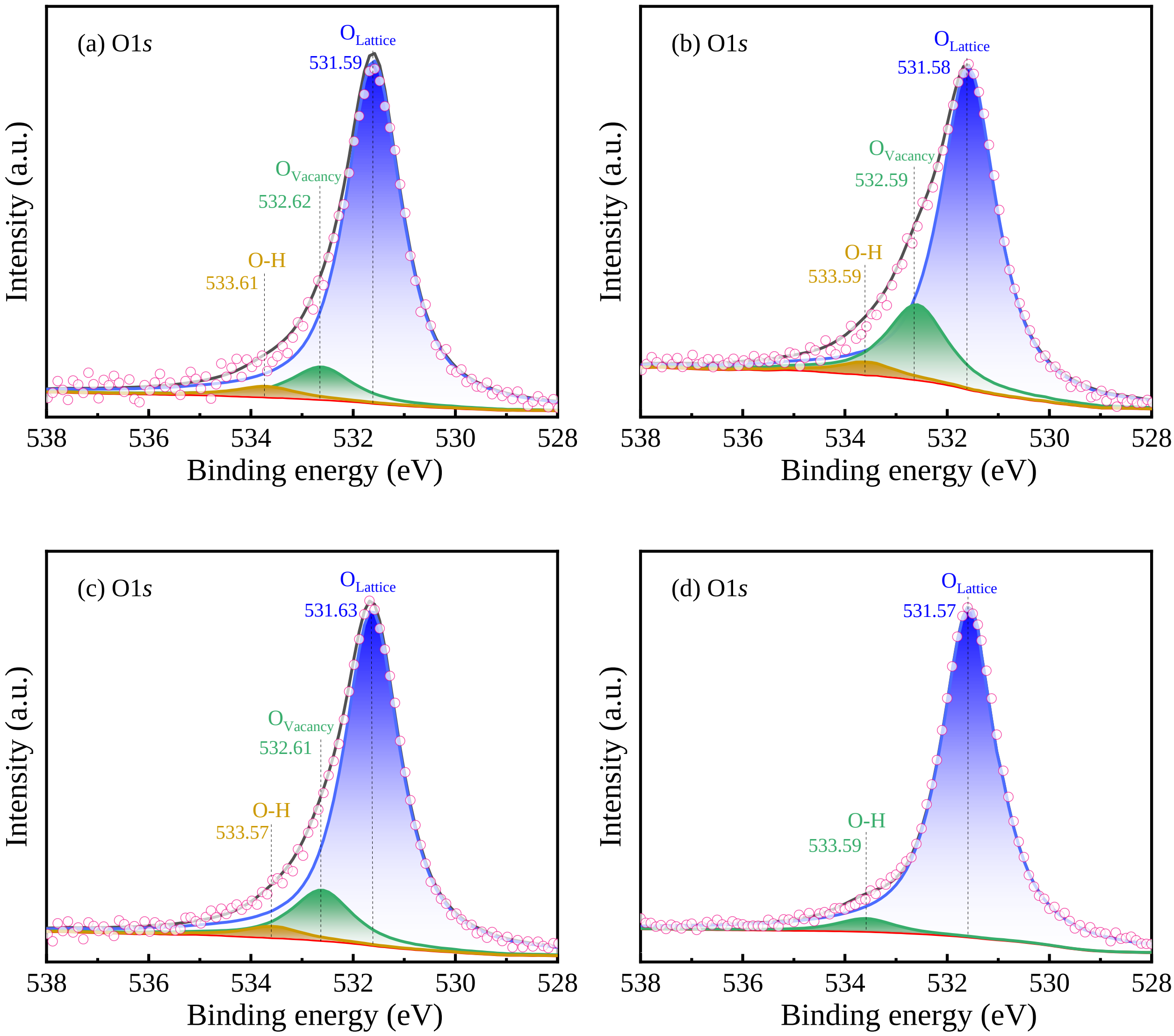

Fig. S1 O1s spectrums for (a) Ag/S-Bi_2O_3-1, (b) Ag/S-Bi_2O_3-2, (c) Ag/S-Bi_2O_3-4, and (d) Bi_2O_3.

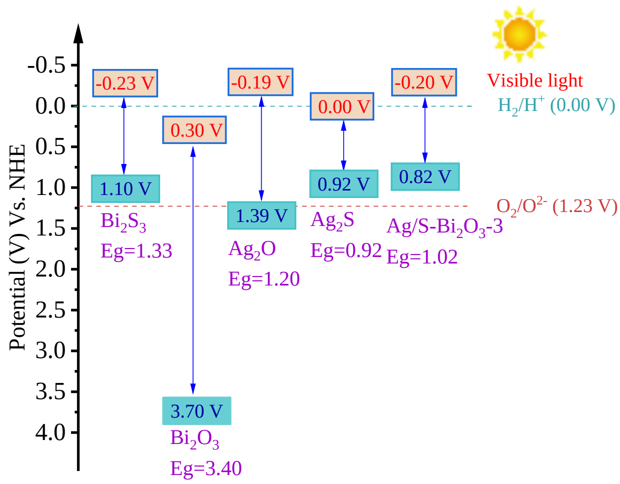

Fig. S2 Schematic band structure diagrams for Bi_2S_3, Bi_2O_3, Ag_2O, Ag_2S and Ag/S-Bi_2O_3.

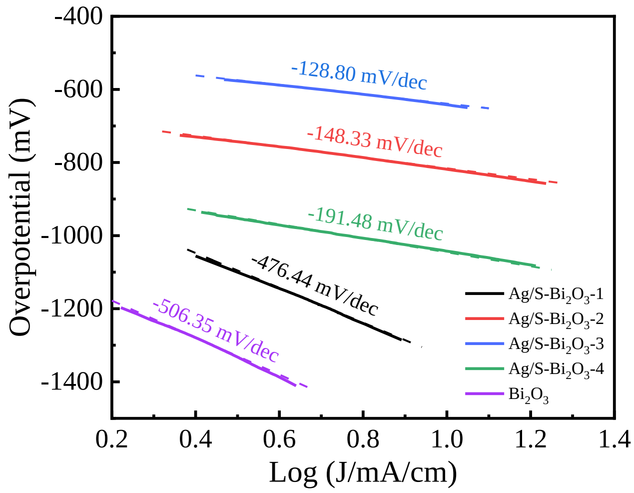

Fig. S3 Tafel slope of Ag/S-Bi_2O_3 and Bi_2O_3 catalysts

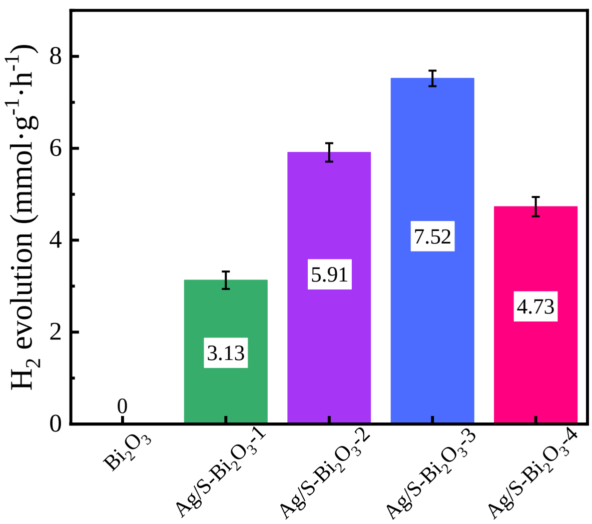

Fig. S4 Photocatalytic hydrogen evolution with the variation of time

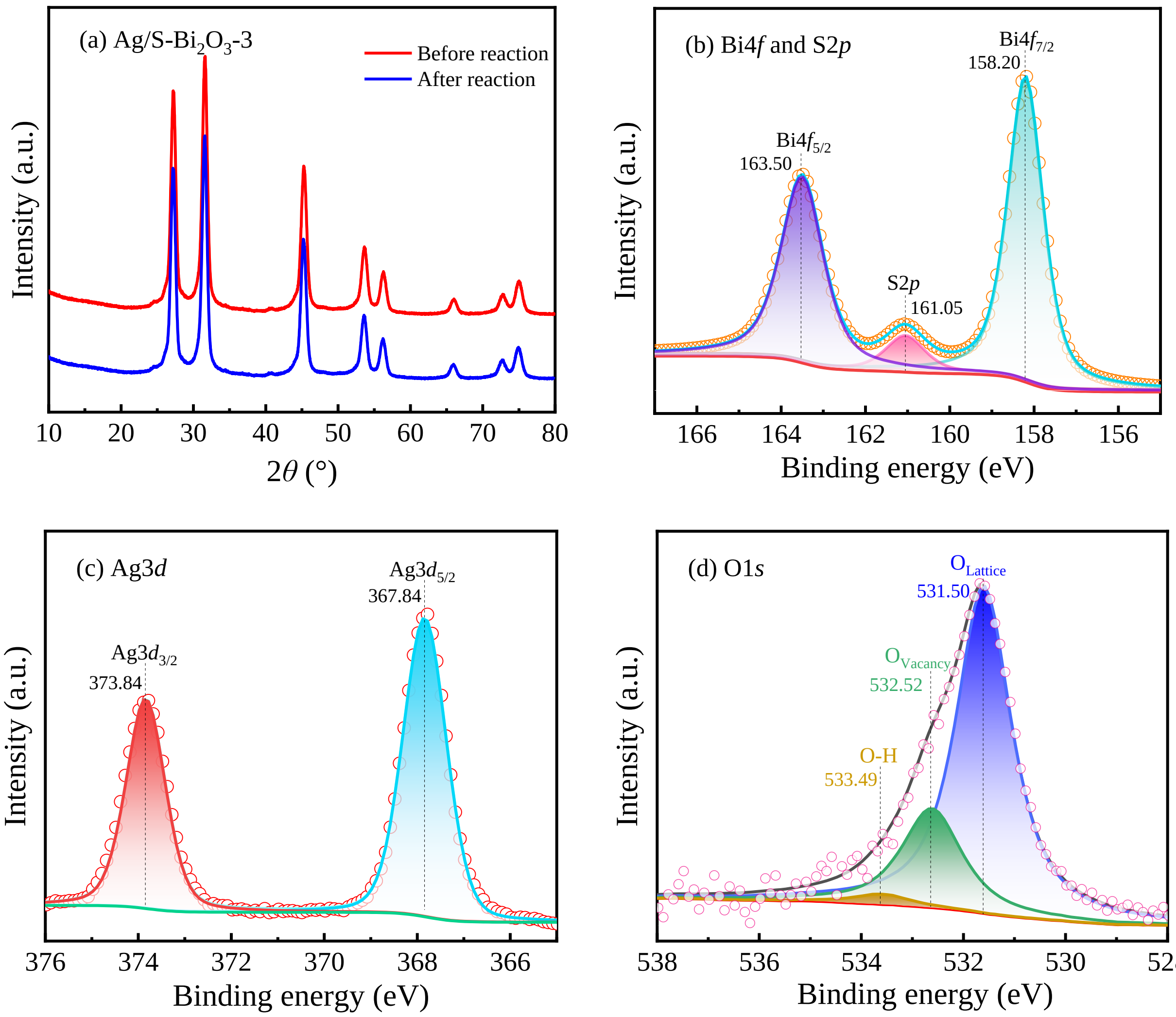

Fig. S5 (a) XRD patterns of Ag/S-Bi_2O_3-3 after reusability reaction 6 times. XPS analyses for (b) Bi 4f and S 2p, (c) Ag 3d, and (d) O 1s.

Table S1 XPS composition, V_O (%), crystal, and S_{BET} analyses of Ag/S-Bi_2O_3 and Bi_2O_3 catalysts

Catalyst	Atomic percentage/%				V_O (%)	Crystal size (nm)	S_{BET} (m^2/g)	Pore volume (cm^3/g)
	Bi	Ag	S	O				
Ag/S-Bi_2O_3-1	21.33	18.47	13.51	46.69	6.61	17.4	38.9	0.291
Ag/S-Bi_2O_3-2	21.02	18.69	14.92	45.37	11.65	15.6	39.8	0.306
Ag/S-Bi_2O_3-3	21.49	18.28	15.64	44.59	15.70	11.3	40.5	0.312
Ag/S-Bi_2O_3-4	21.52	18.14	16.73	43.61	9.74	10.7	39.7	0.298
Bi_2O_3	38.31	N/A	N/A	61.69	N/A	32.9	27.1	0.171
After reaction Ag/S-Bi_2O_3-3	20.83	19.17	15.03	44.97	15.49	11.7	39.7	0.307

Table S2 Elements contents from SEM-EDS analysis for BiAgSO and Bi_2O_3 catalysts

Catalyst	Bi	Ag	S	O
Ag/S-Bi_2O_3-1	22.36	17.63	16.09	43.92
Ag/S-Bi_2O_3-2	22.17	17.54	15.94	44.35
Ag/S-Bi_2O_3-3	22.56	17.19	14.91	45.34
Ag/S-Bi_2O_3-4	22.49	17.58	13.42	46.51
Bi_2O_3	38.18	N/A	N/A	61.82

Table S3 XRF chemical elements composition of Ag/S-Bi_2O_3 and Bi_2O_3 catalysts

Catalyst	Bi	Ag	S	O
Ag/S-Bi_2O_3-1	21.11	18.07	17.09	43.73
Ag/S-Bi_2O_3-2	21.20	18.15	16.24	44.41
Ag/S-Bi_2O_3-3	20.88	18.46	15.31	45.35
Ag/S-Bi_2O_3-4	20.48	18.50	14.42	46.60
Bi_2O_3	38.26	N/A	N/A	61.74

Table S4 Reports on PHER performance over Bi-based and oxysulfide catalysts under visible light

Catalyst	Sacrificial agent	Light source	AQE(%)	PHER rate (mmol/g/h)	Refs.
g-C_3N_4/Au/$BiVO_4$	10 vol% triethanol amine	300 W Xe	N/A	2.986	[4]
BiOBr/Bi_2S_3	Na_2S/Na_2SO_3	300 W Xe	N/A	1.03	[5]
ZnO/Ag/Bi_2S_3	Na_2S/Na_2SO_3	250 W Hg	1.1 (420 nm)	0.218	[6]
Bi_2S_3/MoS_2/TiO_2	Na_2S/Na_2SO_3	250 W Xe	N/A	2.23	[7]
Bi_2S_3/WO_3	5 vol% glycerol	Visible light	2.99 (450±5 nm)	9.91	[8]
FeS_2/Bi_2S_3	Na_2S/Na_2SO_3	300 W Xe	12.1 (420 nm)	16.8	[9]
Bi/Bi_2MoO_6-MoS_2	5 vol% triethanol amine	150 W Xe	15.8 (>420 nm)	2.185	[10]
BSxBWO	10 vol% triethanol amine	250 W Xe	N/A	0.92	[11]
Bi_2S_3/TiO_2	50 vol% methanol	300 W Xe	N/A	2.46	[12]
CdS/Bi_2S_3	Na_2S/Na_2SO_3	300 W Xe	N/A	0.54	[13]
Bi/ZCS	Na_2S/Na_2SO_3	300 W Xe	31.5 (420 nm)	109	[14]
Bi_2O_3/$BiVO_4$	Na_2S/Na_2SO_3	Visible light	N/A	0.171	[15]
Bi/Bi_5O_7I/Sn_3O_4	20 vol% methanol	300 W Xe	N/A	0.326	[16]
Bi_5O_7Br/Ti_3C_2	40 vol% methanol	300 W Xe	N/A	0.079	[17]
Ag/S-Bi_2O_3	Na_2S/Na_2SO_3	300 W Xe	8.67 (420 nm)	7.52	This work

References:

[1] C. Imparato, G. Iervolino, M. Fantauzzi, C. Koral, W. Macky, M. Kobielusz, G. D'Errico, I. Rea, R.D. Girolamo, L.D. Stefano, A. Andreone, V. Vaiano, A. Rossi, A. Aronne, Photocatalytic hydrogen evolution by cocatalyst free TiO_2/C bulk heterostructures synthesized under mild conditions, *RSC Adv.*, 10 (2020) 12519-12534.

[2] M.S. Nasir, G. Yang, I. Ayub, S. Wang, W. Yan, Tin diselinide a stable co-catalyst coupled with branched TiO_2 fiber and g-C_3N_4 quantum dots for photocatalytic hydrogen evolution, *Appl. Catal. B-Environ.*, 270 (2020) 118900.

[3] U. Bharagav, N.R. Reddy, V.N. Rao, P. Ravi, M. Sathish, M.V. shankar, T.M. Aminabhavi, R.R. Kakarla, M.M. Kumari, Z-scheme driven photocatalytic activity of CNTs-integrated Bi_2S_3/WO_3 nanohybrid catalysts for highly efficient hydrogen evolution under solar light irradiation, *Chem. Eng. J.*, 465 (2023) 142886.

[4] R. Muthukumar, G. Balaji, S. Vadivel, The charge transfer pathway of g-C_3N_4 decorated Au/Bi(VO_4) composites for highly efficient photocatalytic hydrogen evolution, Int. J. Hydrogen Energ., 48 (2023) 23856-23865.

[5] C.-J. Chang, C.-L. Huang, Y.-H. Yu, M.-C. Teng, C. Chiang, Y.-G. Lin, Electron transfer dynamics and enhanced H_2 production activity of hydrangea-like BiOBr/Bi_2S_3-based photocatalysts with Cu-complex as a redox mediator, *Appl. Surf. Sci.*, 576 (2021) 151870.

[6] S. Mandal, R. Ananthakrishnan, Double effects of interfacial Ag nanoparticles in a ZnO multipod@Ag@Bi_2S_3 Z-Scheme photocatalytic redox system: Concurrent tuning and improving charge-transfer efficiency, *Inorg. Chem.*, 59 (2020) 7681-7699.

[7] Q.A. Drmosh, A. Hezam, A.H.Y. Hendi, M. Qamar, Z.H. Yamani, K.Byrappa, Ternary $Bi_2S_3/MoS_2/TiO_2$ with double Z-scheme configuration as high performance photocatalyst, *Appl.*

Surf. Sci., 499 (2020) 143938.

[8] U. Bharagav, N.R. Reddy, V.N. Rao, P. Ravi, M. Sathish, M.V. Shankar, T.M. Aminabhavi, R.R. Kakarla, M.M. Kumari, Z-scheme driven photocatalytic activity of CNTs-integrated Bi_2S_3/WO_3 nanohybrid catalysts for highly efficient hydrogen evolution under solar light irradiation, *Chem. Eng. J.*, 465 (2023) 142886.

[9] M. Li, J. Sun, G. Chen, S. Yao, B. Cong, P. Liu, Construction photothermal/pyroelectric property of hollow FeS_2/Bi_2S_3 nanostructure with enhanced full spectrum photocatalytic activity, *Appl. Catal. B-Environ.*, 298 (2021) 120573.

[10] R.K. Chava, N. Son, M. Kang, Surface engineering of CdS with ternary Bi/Bi_2MoO_6-MoS_2 heterojunctions for enhanced photoexcited charge separation in solar-driven hydrogen evolution reaction, *Appl. Surf. Sci.*, 565 (2021) 150601.

[11] R. Bariki, Y.P. Bhoi, S.K. Pradhan, S. Panda, S.K. Nayak, K. Das, D. Majhi, B.G. Mishra, Oxygen defect rich Bi_2S_3/SnS_2/Bi-self doped $Bi_2W_2O_9$ multijunction photocatalyst for enhanced degradation of methyl parathion and H_2 evolution, *Sep. Purif. Technol.*, 324 (2023) 124509.

[12] H. Lin, K. Zhang, G. Yang, Y. Li, X. Liu, K. Chang, Y. Xuan, J. Ye, Ultrafine nano 1T-MoS_2 monolayers with NiO_x as dual co-catalysts over TiO_2 photo harvester for efficient photocatalytic hydrogen evolution, *Appl. Catal. B-Environ.*, 279 (2020) 119387.

[13] M. Li, H. Yao, S. Yao, G. Chen, J. Sun, Vacancy-induced tensile strain of CdS/Bi_2S_3 as a highly performance and robust photocatalyst for hydrogen evolution, *J. Colloid Interface Sci.*, 630 (2023) 224-234.

[14] G. Yang, T. Chen, H. Liu, C. Xing, G. Yu, X. Li, Bi-doped twin crystal $Zn_{0.5}Cd_{0.5}S$ photocatalyst for highly efficient photocatalytic hydrogen production from water, *Appl. Surf. Sci.*, 615 (2023) 156393.

[15] F. Shafiq, M.B. Tahir, A. Hussain, M. Sagir, J.U. Rehman, I. Kebaili, H. Alrobei, M. Alzaid, The construction of a highly efficient p-n heterojunction Bi_2O_3/$BiVO_4$ for hydrogen evolution through solar water splitting, *Int. J. Hydrogen Energ.*, 47 (2022) 4594-4600.

[16] L. Xu, W. Chen, S. Ke, S. Zhang, M. Zhu, Y. Zhang, W. Shi, S. Horike, L. Tang, Construction of heterojunction Bi/Bi_5O_7I/Sn_3O_4 for efficient noble-metal-free Z-scheme photocatalytic H_2 evolution, *Chem. Eng. J.*, 382 (2020) 122810.

[17] F. Xie, Q. Xi, H. Li, X. Jian, J. Liu, X. Zhang, Y. Wang, R. Li, C. Fan, Two-dimensional/two-dimensional heterojunction-induced accelerated charge transfer for photocatalytic hydrogen evolution over Bi_5O_7Br/Ti_3C_2: Electronic directional transport, *J. Colloid Interface Sci.*, 617 (2022) 53-64.